



An-Najah National University

Faculty of Engineering

Graduation project 1

Self-Leveling Base

Prepared By: Khalid Jaara

Supervised By: Dr. Falah Mohammed

ABSTRACT

To be able to measure and compensate for imbalance is essential for stabilizing mechanisms. The technique is applied in everything from self-stabilizing cameras to helicopters and noise reducing equipment. This report describes the development of a self-stabilizing platform, and includes theory about sensors, filters and motor modelling, and also practical tests. The purpose is to answer how the system will behave when a load is placed asymmetrically on the platform and if it is possible to compensate for the imbalance that occurs. The tilt of the platform is measured by an IMU, a sensor combining accelerometers and gyroscopes. A Kalman filter is used to combine the data. From this a signal, with noise levels within the requirements, was obtained. A theoretical model was set up for the system. The system was modelled based on a load of 125g placed in the center of the platform. Two DC-motors compensate for the tilt around each axis. The motors are seen as separate sub systems and are controlled independently. The system is controlled by two PID-controllers which were designed based on the requirements that were set up regarding speed and stability. A short rise time and a small overshoot were essential to be able to minimize the torque on the motor shafts. The same requirements were set for each sub system. The chosen PID-parameters acquired a system which at a step input of 11.4° had a rise time of 0.75s, a settling time of 1.35s and an overshoot of 0.8%. The demonstrator that was constructed was put through a number of tests to answer the research questions. By placing the load at different distances from the center, the theoretical model was examined from its sensitivity to deviations. The test showed that a farther distance

between the load and the center corresponded to a greater angular fluctuation and a longer settling time.

CONTENTS

- ABSTRACT** 2
- COMTENTS**
- NOMENCLATURE** 6
- 1.INTRODUCTION** 9
 - 1.1 BACKGROUND 9
 - 1.2 PURPOSE 9
 - 1.3 SCOPE 10
 - 1.4 METHOD 10
 - 1.5 RELATED PROJECTS 11
- 2.THEORY** 12
 - 2.1 STABILIZING PLATFORMS 12
 - 2.2 THE IMU 13
 - 2.3 KALMAN FILTER 13
 - 2.4 PID 14
 - 2.5 THE ELECTRICAL CIRCUIT OF A DC-MOTOR 15
- 3.DEMONSTRATOR** 16
 - 3.1 PROBLEM FORMULATION 16
 - 3.2 ELECTRONICS 17
 - 3.2.1 Microcontroller 17

3.2.2 Motor and gearheads	17
3.2.3 Motor driver	17
3.2.4 IMU	18
3.3 SOFTWARE	18
3.4 HARDWARE	19
3.4.1 Motor holders	19
3.4.2 Motor arm	19
3.4.3 Upper platform	20
3.4.4 Naves	20
4.CALCULATIONS	21
4.1 CALCULATIONS FOR THE MOTORS	21
4.1.1 Motor A	22
4.1.2 Motor B	22
4.1.3 Calculations	23
4.2 STEP RESPONSE	24
4.3 TESTS	25
4.3.1 Test of Kalman filter	25
4.3.2 Test with asymmetrically placed load	25
4.4 RESULTS	26
4.4.1 Noise with Kalman filter	26
4.4.2 Step info	27

4.4.3 Asymmetrically placed load	27
5. DISCUSSION AND CONCLUSION	29
5.1 DISCUSSION	29
5.1.1 Kalman filter	29
5.1.2 PID and step response	29
5.1.3 Asymmetrically placed load	29
5.1.4 Possible error sources	30
5.2 CONCLUSIONS	30
6. RECOMMENDATIONS AND FUTURE WORK	31
6.1 RECOMMENDATIONS	31
6.2 FUTURE WORK	31
REFERENCES	33

NOMENCLATURE :

Here the symbols and nomenclature used in the project are described in the order they appear in the report.

Symbols :

Symbol	Description	
X_t	State matrix at time t	
X_{t-1}	State vector at time t-1	
θ	Angle (rad)	
$\dot{\theta}$	Angle velocity (rad/s)	
F_t	State transition matrix	
u_t	Control input vector for Kalman filter	
b_t	Control input matrix	K_P Proportional part parameter
w_t	Vector containing process noise terms at time t	
e	static error	
u	input signal	
K_I	Integrative part parameter	
K_D	Derivative part parameter	
R	Motor resistance (Ω)	
L	Motor Inductance (H)	
b	Dynamic friction constant (Nm·s)	
J_{rotor}	Moment of inertia for the rotor ($kg \cdot m^2$)	

J_A	Moment of inertia for the parts mounted on motor A ($\text{kg}\cdot\text{m}^2$)
J_B	Moment of inertia for the parts mounted on motor B ($\text{kg}\cdot\text{m}^2$)
K_e	Voltage constant for the motor ($\text{V}\cdot\text{s}/\text{rad}$)
K_t	Torque constant (Nm/A) T
Motor torque (Nm)	
e_{emf}	Back emf
m	Mass of the load (kg)
l	Distance between motor shaft and center of the load (m)
θ''	Angle acceleration (rad/s^2)
F_c	Static friction constant

Abbreviations :

IMU	Inertial measurement unit
I ² C	Inter-Integrated Circuit
MATLAB	Matrix Laboratory
PID	Proportional-integral-derivative
PWM	Pulse-width modulation
ABS	Acrylonitrile butadiene styrene
CAD	Computer Aided Design

1. INTRODUCTION

This chapter discusses the background of the project and its purpose. It states the scope and the limitations behind the project, as well as the methods used to acquire the result.

1.1 Background

Today many industries are dependent on stabilizing mechanisms. The technique is used in a wide range of products, from camera stabilizing devices (Gosselin, StPierre, 2003) to helicopters (Institut für Theoretische Elektrotechnik und Systemoptimierung, 2006) and medical devices when performing precise surgery (Journal of Cardiothoracic and Vascular Anesthesia, 2002, 685–690). One field of application is the stabilizing platform, which for example is used in self-leveling equipment like anti-motion sickness chairs (David E. Grober, US 7490572 B2). The stabilizing platform, which purpose is to compensate for angular fluctuation, exists in many forms. The idea is to measure the angle which the platform is tilted, and then compensate for this by a motor. The angle can be measured by a potentiometer or by more advanced sensors, and the motors can be anything from servo motors to step motors and DC-motors (Liu, Qiang Zhu and Howe, 2006).

1.2 Purpose

The purpose of this report is to analyze how feedback-control can be used along with accelerometers and gyroscopes to stabilize a platform. In this project this will be accomplished by an Arduino platform (Arduino, 2015) and an IMU (a sensor with accelerometers and gyroscopes) which gives feedback to two DC-motors.

The purpose is also to study how the system reacts to both a symmetrically and an asymmetrically placed load. To simplify the theoretical model the considered load was put in the middle of the platform. This simplification made it essential to test the model on a demonstrator.

Two research questions were to be answered:

- How would the system reply to a load put asymmetrically on the platform?

- Can the imbalance be compensated for?

1.3 Scope

The Open-Source Arduino-platform has contributed in making the use of stabilization tools like accelerometers and gyros easier and more approachable. The filter used for filtering the data from the IMU was collected from an open source library. Therefore the theory behind is covered very briefly. Focus was put on testing and verifying the output from the sensor to determine if the setup was good enough for the project.

Also the communication bus I2C between the sensor and the Arduino is from an open source library and is not explained further.

This report covers how to control two motors independently to keep a desired angular output. A lot of effort has been put to make the theoretical model of the system as correct as possible, to be able to implement an efficient feedback control on the demonstrator. Therefore the calculations to find a transfer function from angle to voltage are described in detail.

This report follows the scope of a Bachelor thesis at KTH and corresponds to 10 weeks of work.

1.4 Method

By analyzing the mechanics for the problem, a theoretical model was made of the system. The model was used to design a feedback control which fulfilled the demands that were set up for the platform.

A demonstrator of the system was built to be able to test the theoretical model in reality. Tests were made on the demonstrator by using a set load which was put on different distances from the center of the platform. The data from the tests was evaluated in MATLAB.

1.4 Related projects

Two other projects were used as inspiration for this project.

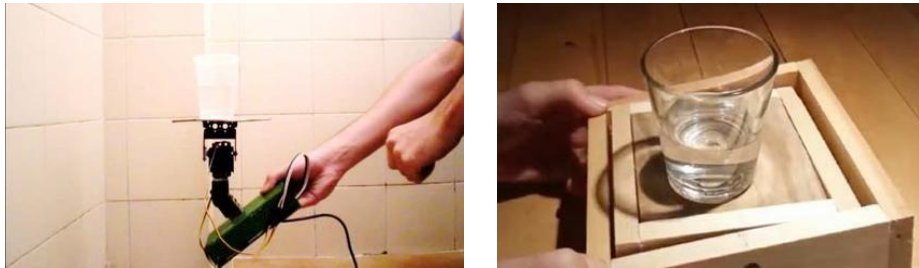


Figure 1. a) A similar project where two servos compensate for the tilt (Rivello, 2011).
b) The project Coffee Mate (Because We Can! labs, 2014).

One existing project where a platform is stabilized by two servo motors is shown in Figure 1 a. An IMU is placed in the box at the bottom together with an Arduino and the servos move according to the measured angles when the box is tilted. This model does not measure the tilt of the upper platform, and therefore no feedback control is implemented.

Another project is the CoffeeMate seen in Figure 1 b, a self-stabilizing platform built to be used on a boat. This project also uses an IMU and two servo motors but the difference in height between the servomotors and the platform is smaller, and thereby the fluctuation of the platform is reduced.

2. THEORY

The theory in this chapter describes the essential parts to be able to understand and answer the research questions that were set in the project.

2.1 Stabilizing platforms

The tilt of a platform can be measured in a variety of ways. A possible solution is to use a potentiometer which has a definite range of rotation. Another option is to use a rotary encoder (Ruderman et al, 2008). This measures the rotation of the motor shaft and in contrast to a potentiometer infinite rotation is possible. Another method is to use an accelerometer, or combine it with a gyroscope (Paller, 2012).

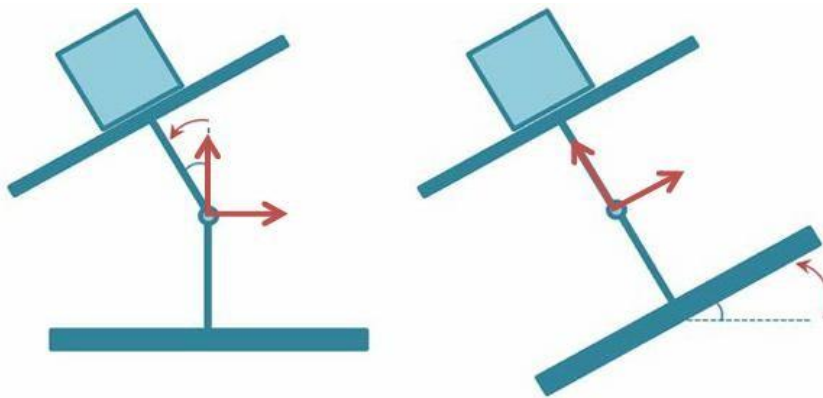


Figure 2. a) The reference plane of the motor is unaffected by the tilt.

b) The reference plane is affected by the tilt.

The platform in the project is supposed to stay horizontal both when disturbances is implemented directly on the platform (Figure 2 a) or on its base where the motors are mounted (Figure 2 b). This means that the tilt cannot be measured with a device which is connected to a movable reference plane. This is the case with both an encoder and a potentiometer. A sensor like an accelerometer measures the gravity with the earth as reference which makes it more suitable for this project.

2.2 THE IMU

An accelerometer measures the amount of static acceleration due to gravity, and with this information it is possible to determine the angles that it is tilted in relation to the earth. The accelerometer has no accumulated error but it has gravity component problem due to that it measures the sum of gravity and motion acceleration (Paller, 2012). One way to separate these two is to use a gyroscope.

A gyroscope measures rotation around three axis, i.e. angular velocity. A Gyroscope is not sensitive to gravity and is a good complement to an accelerometer. The gyro has an accumulated error, but no problem with gravity acceleration.

The weaknesses of both sensors can be compensated for by combining them (Dimension Engineering, 2015). The combination is called an IMU which is a fusion of an accelerometer and a gyroscope.

4.3 Kalman filter

The IMU supplies data, which in its raw form can be noisy. This demanded a filter that would both eliminate measurement noise and generate an accurate output.

The Kalman filter is used to filter the raw data the sensors generate to useful input to the system. It's a filter that uses both sensor measurements and the physical laws of motion to generate an estimated value. (Faragher, Ramsey, 2012)

The Kalman filter uses different states where the value of the previous state is included in the estimation of the next one. The estimation often becomes more accurate since the filter operates recursively with three states in the calculations, the past, the present and the future (Kleeman, L. 1996). The model assumes that the state of a system at a time t evolves from the prior state at time $t-1$, and is described in Equation 1.

$$X_t = F_t X_{t-1} + B_t u_t + w_t \quad (1)$$

Where X_t is the state matrix at time t , and X_{t-1} is the state vector at time $t-1$. The state matrix is given by

$$X_t = \begin{bmatrix} \theta \\ \dot{\theta}_b \end{bmatrix}_t \quad (2)$$

This means the output of the filter will be the angle θ and the bias $\dot{\theta}_b$ based on the measurements from the accelerometer and gyroscope.

The F matrix is the state transition model, applied on the previous state X_{t-1} . Here F is

$$F = \begin{bmatrix} 1 & -\Delta t & 0 & 1 \\ 0 & 1 & 0 & 0 \end{bmatrix} \quad (3)$$

Further on, u_t is the control input vector, and this depends on the measurements of the gyroscope in degrees per second. This is multiplied by the B matrix, the control-input model, defined as

$$B = \begin{bmatrix} \Delta t \\ 0 \end{bmatrix} \quad (4)$$

and w_t is a vector containing the process noise at time t.

The filter uses covariance matrices as a measurement of the similarity in behavior or the linear relationship between variables. A positive covariance for X and Y means that when X is increasing the same will happen to Y (Weisstein, 2015). This is used to determinate the Kalman gain, which is a factor of how much a measurement should be trusted. A high gain means that the filter method will relate more on measurements and at a low gain the filter will trust more on the filter model itself.

2.4 PID

PID-control is a very common feedback-control (Åström and Murray, 2004) which uses the error e (the difference between a desired set point and a measured value) to calculate the input signal u to the system.

$$u(t) = K_P e(t) + K_I \int_0^t e(t) dt + K_D \frac{d}{dt} e(t) \quad (5)$$

By varying the parameters K_P , K_I and K_D in Equation 5 the controller can be tuned in infinite number of ways. Very briefly, increasing K_P will improve the speed of the system but reduce the stability. By increasing K_I it is possible to eliminate the steady state error but also risking the stability. The K_D parameter can improve the stability of the system by letting the input of the system depend on the derivate of the error but makes the system more sensitive to measurement noise (Glad och Ljung, 2014, 53).

2.5 The electrical circuit of a DC-motor

The following model of the electrical circuit was inspired by a calculation example (MathWorks, 2012). The model describes how the angular velocity of the motor shaft depends on the back electromotive force, back emf.

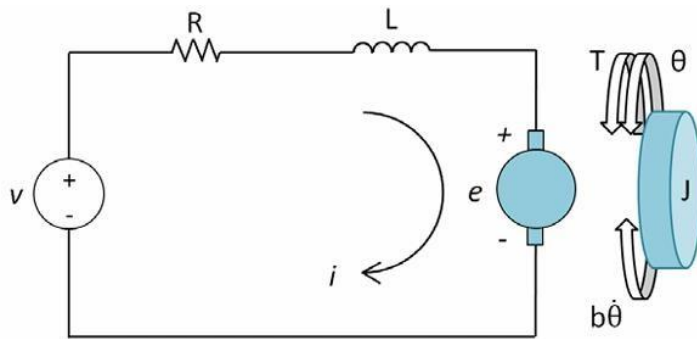


Figure 3. The electrical circuit

In Figure 3 the electrical circuit is shown, where R is the electric resistance, L is the electric inductance, e is the back emf, v is the voltage, T is the motor torque. Further on θ is the angle, b is the motor dynamic friction constant, $\dot{\theta}$ is the angular speed and J is the moment of inertia.

Kirchhoff's law of voltage (Johansson et al, 2010, 1-14) gives

$$L \frac{di}{dt} + Ri = V - e \quad (6)$$

Where the back emf e_{emf} is given by (Johansson et al, 2010, 7-12)

$$e_{emf} = K_e \dot{\theta} \quad (7)$$

where K_e is the voltage constant for the motor.

3. DEMONSTRATOR

This chapter discusses both the process to make the demonstrator, as well as the finished result. It contains information about the hardware, the software and the electronics used in the project.

3.1 Problem formulation

When constructing the demonstrator the following was considered:

- The construction must minimize the torque on the motor shafts
- Sensor noise will affect the system more if the distance from the motors to the platform is big
- The arms cannot be too short since the platform must be able to move freely without interfering with other parts
- The IMU must be placed as high as possible to make the accelerometer more sensitive of movements
- The weight of the components should be as low as possible to minimize the moment of inertia

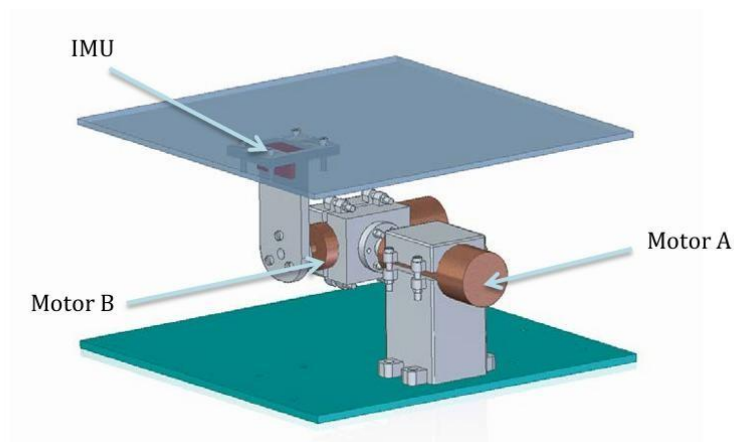


Figure 4. The demonstrator

The design of the demonstrator is shown in Figure 4 where motor A, motor B and the IMU are shown.

3.2 Electronics

3.2.1 Microcontroller

The Arduino Uno (Arduino, 2015) is an open source platform based on the ATmega32 microcontroller (Atmel, 2015). The platform contains 14 digital pins and 6 analog pins. It has a clock speed of 16 MHz. The Arduino is used with its own interface software based on the C and C++ code language.

3.2.2 Motors and gearheads

Two Faulhaber 2842 006C DC-motors (Michigan Tech, 2015) were used to compensate for the tilt of the platform. They were able to handle a nominal voltage of 6V and a continuous current of 1.55A.

The two motors were used with two planetary gearheads from the Faulhaber 23/1 series with a ratio of 14:1 (Faulhaber, 2015).

	Parameter	Value	Source
Resistance	R	1.6 Ω	<i>Data sheet</i>
Induction	L	145 μH	<i>Data sheet</i>
Dynamic friction constant	b	9.1496e-4 Nm·s	<i>Calculated (See Appendix A)</i>
Rotor inertia	J_{rotor}	9.7026e-7 kg m ²	<i>Data sheet</i>
Moment of inertia for motor A	J_A	1.066e-3 kg m ²	<i>Solid Edge CAD</i>
Moment of inertia for motor B	J_B	0.991e-3 kg m ²	<i>Solid Edge CAD</i>
Voltage constant for the motor	K_e	1.150 mV/rpm	<i>Datasheet</i>
Motor torque constant	K_t	10.9 mNm/A	<i>Datasheet</i>

Table 1. Motor specifications (Michigan Tech, 2015 and Faulhaber, 2015) The motor specifications can be found in Table 1. The dynamic friction constant was determined by an analysis which is described in Appendix A.

3.2.3 Motor driver

The dual motor driver Keyes L298 (Arduino, 2015) was used to control both the speed and direction of the motors. The motor driver made it possible to control both motors independently using PWM signals. It was able to handle voltage up to 46V and a total current up to 4A. This was enough for the chosen DC-motors. The motor driver can handle a PWM-frequency up to 40 kHz and this was set to 20kHz to get rid of unwanted noise from the motors.

3.2.4 IMU

The sensor used was the MPU-9150 (InvenSense, 2012) with both gyroscope and accelerometers for three axis. The gyroscope was able to handle a rate of ± 2000 $^{\circ}/s$ but since the angular speed would not be that fast the rate was set to ± 250 $^{\circ}/s$ because of the risk of losing accuracy with a higher rate. The full scale range of the accelerometer is $\pm 16g$. However it's set to $\pm 2g$ because of the same premises as the rate of the gyroscope.

3.3 Software

The software was divided into the two systems A and B where each subsystem represents a motor which compensates for the tilt around either the x-axis (θ_B) or y-axis (θ_A) as seen in Figure 5. System A and system B are controlled independently with separate PID- and motor control.

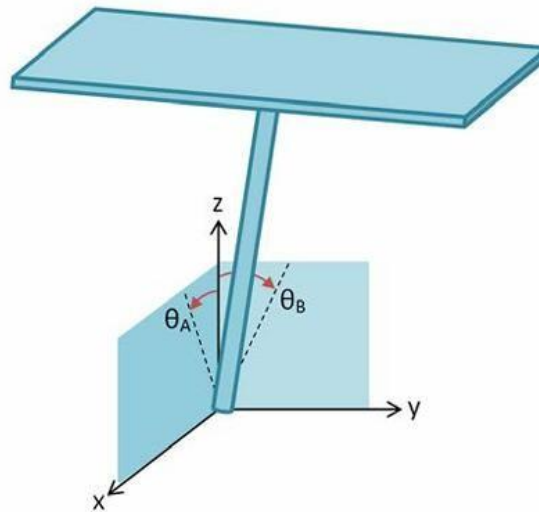


Figure 5. θ_A is the tilt around the y-axis, θ_B is the tilt around the x-axis.

The sensor data is filtered through a Kalman-filter which has the angles θ_A and θ_B as output. An open-source Kalman-filter was used (Lauszus, 2015). The filter output gives input to the PID-controllers by calculating the errors (with a reference angle $Ref_{A,B} = 0^{\circ}$).

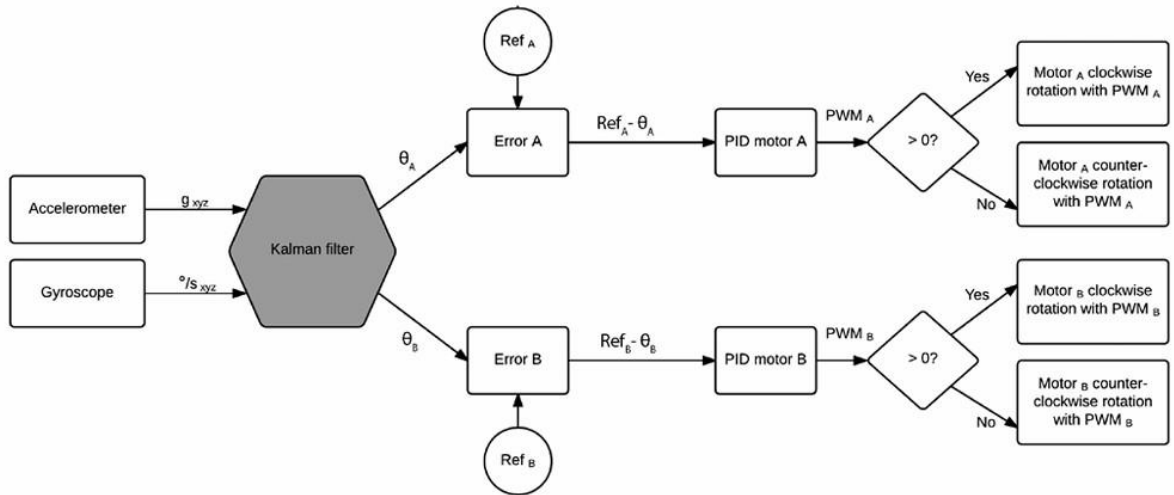


Figure 6. Flow chart of the software system.

The PID uses the errors to calculate which PWM signals to send to the motors according to Equation 5. It has an anti-windup addition to limit the integral part from growing too big. The PWM-signal calculated from the PID makes it possible to control both speed and direction of the motors to compensate for any tilt of the platform. A flow chart of the process is shown in Figure 6.

3.4 Hardware

The demonstrator was built according to the 3D-model shown in Figure 4. Most of the parts were self-manufactured.

3.4.1 Motor holders

Motor A was put on a holder which was put on the lower platform containing the Arduino and an H-bridge. A motor holder for motor B was put on the motor shaft of motor A. Motor B was put so that its shaft would always be orthogonal to the shaft of motor A. Both of the motor holders were 3D-printed using ABS-plastic.

3.4.2 Motor arm

The arm from motor B to the upper platform was designed with a holder for the sensor, and holes for attaching the platform. It was also 3D-printed with ABS-plastic.

3.4.3 Upper platform

The upper platform was made from acrylic glass with a thickness of 2 millimeters. It was mounted on the motor arm so that the center of mass would be placed above the axis for both motor A and B. This was done to eliminate the torque from an object placed at the center of the platform.

3.4.4 Naves

Pre-manufactured aluminum naves (Electrokit, 2015) were used to transfer the torque from the motor shaft with two screws pressing on the flat side of the shaft.

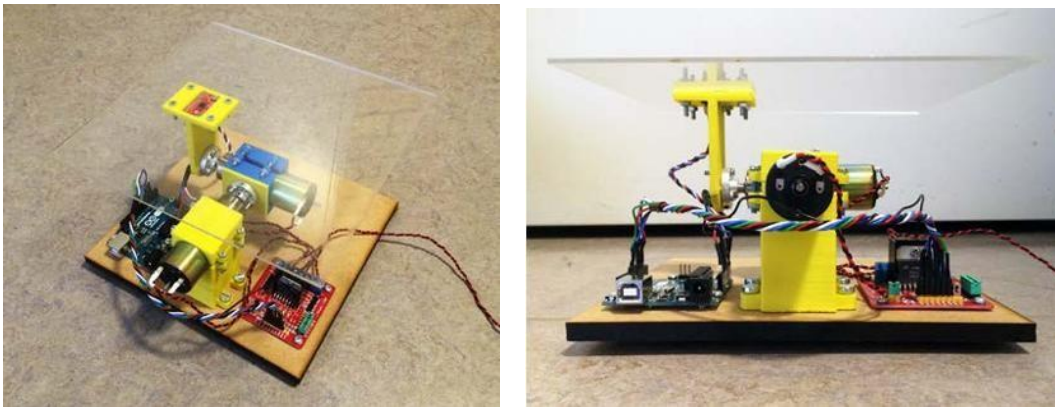


Figure 7. The demonstrator.

4. CALCULATIONS

This chapter contains the calculations made to find the transfer functions for the two motors. Also, the tests to answer the research questions are described as well as the results from these.

4.1 Calculations for the motors

To be able to design a feedback controller for the system, a transfer function was essential to find. Therefore a mechanical model of the system was made. The model is inspired by a calculation example (MathWorks, 2012).

The demonstrator contains two DC-motors which each tilt the platform orthogonal to each other. To simplify the system, each motor is seen as separate sub-system. Different parameters are used for these sub-systems depending on length of arm, mass etc.

Subsystem A corresponds to the movement in the xz-plane, and the rotation around the y-axis. The subsystem B corresponds to movement in the yz-plane, with rotation around the x-axis, as seen in Figure 5.

To separate the two sub systems, the motors are referred to as motor A and motor B.

Motor A is the motor mounted on the lower platform and motor B is the motor which the upper platform and sensor are mounted to. This can be seen in Figure 4.

The model does not contain the static friction in the motor since it is non-linear and not possible to include in the transfer functions. However, the dynamic friction is considered and calculated in Appendix A.

Since the motors compensate for the angular fluctuation continuously the torque which emerges at a small angle is considered small enough to be neglected.

In the calculations an intended load is put in the center of the platform, which will not affect the torque, only the moment of inertia for the system.

4.1.1 Motor A

On the shaft of motor A a holder is mounted where motor B is attached.

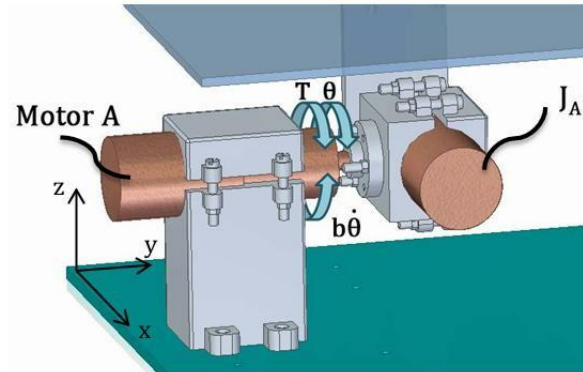


Figure 8. Subsystem for motor A.

The shaft of motor A is balanced when no load is put on the platform. The mechanism for motor A is shown in Figure 8. T is the torque from the motor, θ is the rotation angle, b is the dynamic friction, $\dot{\theta}$ the angular velocity and J_A the inertia for the parts mounted on the shaft.

4.1.2 Motor B

Motor B is attached to the shaft of motor A. An arm is mounted on the shaft of motor B which holds the sensor and supports the platform.

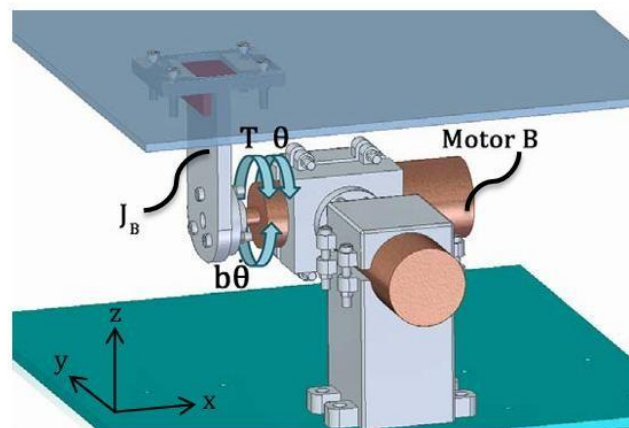


Figure 9. Subsystem for motor B.

The symbols are the same as for motor A, except J_B which is the inertia for the parts mounted on the shaft of motor B. See Figure 9.

4.1.3 Calculations

It is assumed that the magnetic field is constant, and therefore the motor torque is proportional to only the current i by a constant factor K_t which is the motor torque constant. (Johansson et al, 2010, 7-12),

$$T = K_t \cdot I \quad (8)$$

The torque equation for the shaft is given by

$$T - b\dot{\theta} - J\ddot{\theta} = 0 \quad (9)$$

Equation 8 is inserted in Equation 9. The constant K_t and the constant K_e from Equation 7 are after simplification to SI-units the same, and therefore the constant K is used from now on for both constants.

J is the moment of inertia, and is different for the two motors. The inertia for the mounted parts is obtained from the 3D model. The rotor inertia J_{rotor} is found in the data sheet (Faulhaber, 2015). An intended load with a mass m and its center of mass at distance l from the motor axis is included in the calculations. The moment of inertia for this load is calculated as a point mass by using

$$J_{load} = ml^2 \quad (10)$$

By adding the moment of inertia for the moving parts, the rotor inertia and the inertia for the load (Equation 10), a total moment of inertia is acquired for each motor.

After Equation 6 and Equation 9 are Laplace transformed the following equations are obtained

$$KI(s) = bs\theta(s) + Js^2\theta(s) \quad (11)$$

$$LsI(s) + RI(s) = V(s) - Ks\theta(s) \quad (12)$$

The current $I(s)$ is eliminated from Equation 11 and Equation 12 and a new equation is given

$$\frac{1}{Js^2 + bs} \theta(s) = \frac{1}{Ls + R} [V(s) - Ks\theta(s)] \quad (13)$$

The input is the voltage V and the output is the angle θ . From Equation 13 a transfer function can be calculated.

$$P(s) = \frac{\theta(s)}{V} = \frac{K}{(Ls+R)(Js^2+bs)+k_2s} \quad (14)$$

With the plant $P(s)$ from Equation 14 the system behavior can be optimized with feedback control. The plants for motor A and motor B are here on referred to as P_A and P_B .

4.2 Step response

Requirements for the system were set up. A fast system was essential to always keep the load just above the motor shafts to limit the torque. This demanded a rise time under 1 second. A fast system can cause overshoot but the overshoot had to be small to presume the stabilizing abilities of the system. With this considered the desired overshoot was set to less than 2%. A static error up to 1° was allowed since a lower value would risk the stability of the system. The friction between the load and the platform was considered enough to prevent the load from sliding off.

Rise time	< 1 s
Overshoot	< 2 %
Settling time	< 2 s
Steady state error	< 1°

Table 2. System requirements.

The system was modified in MATLAB according to the requirements in Table 2 with a step of 0.2 radians, which equals 11.4° . This was done in the discrete time domain (Pan and Pal, 1995) with a sample time of 50 ms. Both systems had the same requirements.

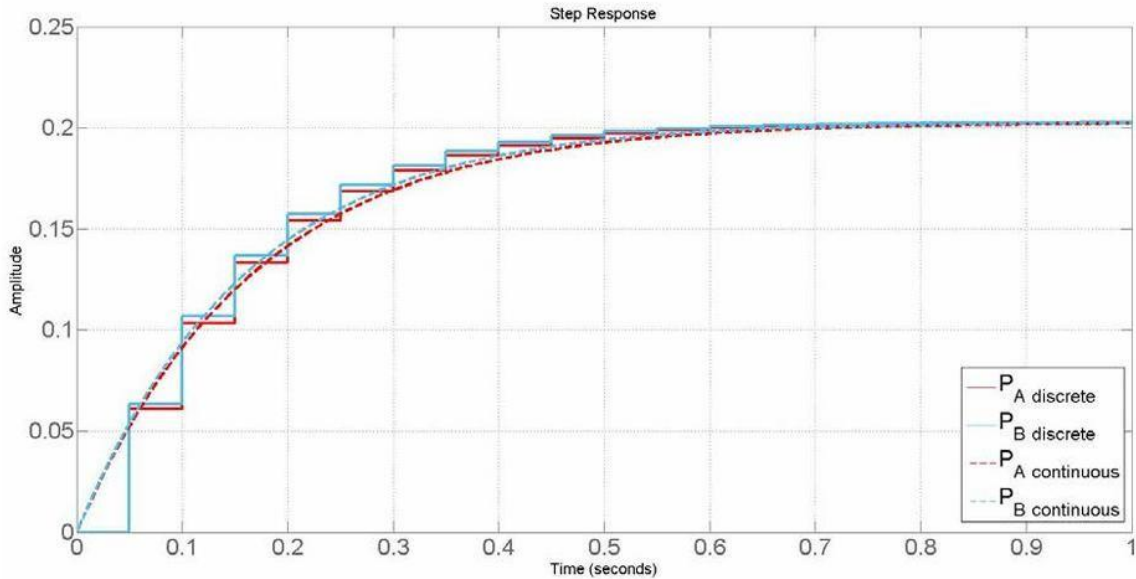


Figure 10. Step response for the two closed systems, in the discrete and in the continuous time domain. The PID-parameters for each motor controller were varied to obtain the step response which can be seen in Figure 10. The two step responses are similar, since the only thing separating them is the moment of inertia. By implementing the PID-parameters in the software, tests could be made with the demonstrator.

4.3 Tests

To be able to answer the research questions testing was necessary. Also, a test was made for the Kalman filter to examine the level of noise in the output.

4.3.1 Test of Kalman filter

A Kalman filter was used to obtain a more reliable output. Still, no filter provides an output free of noise (Faragher, Ramsay, 2012). It was necessary to test how much noise the filtered signal contained.

During the test the sensor was put on a flat surface and was kept still while the filtered angle was measured. The maximum amplitude of noise accepted was set to 0.2° and any amplitude lower than this would fulfill the demands for the project.

4.3.2 Test with asymmetrically placed load

The PID-model was implemented on the demonstrator. Since the model is based on a load placed in the middle of the platform, a test of how well the system compensates for a load put on the platform asymmetrically was accomplished.

A load of 125 grams was put at the center of platform where the center of mass is just above both axes of the motors. This limits the impact of the torque from the load to a minimum which is how the system is modeled. To examine how the system reacts if the load is placed asymmetrically it was moved with even intervals towards the edge of the platform.

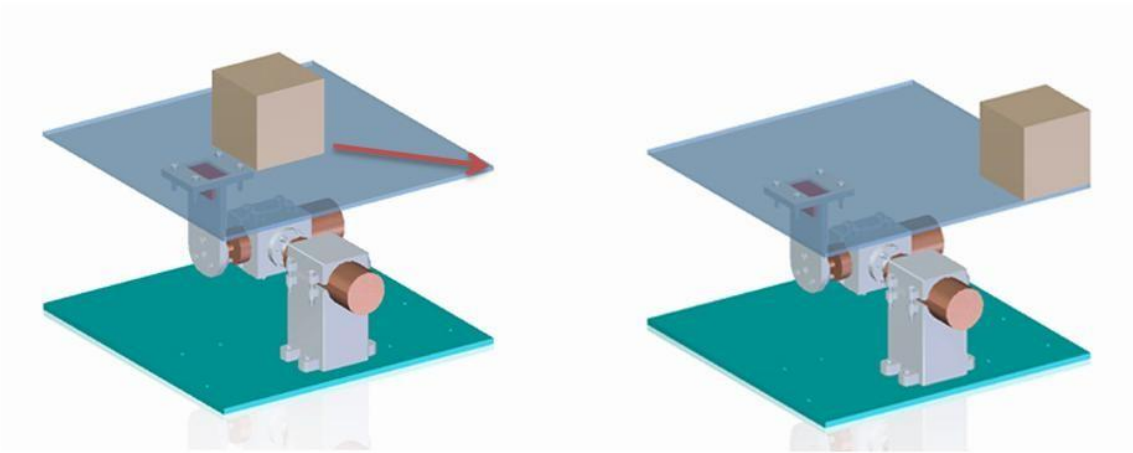


Figure 11. The load was moved from the center to the edge of the platform. The load was put at four different distances from the center (Figure 11). The tilt of the platform was measured at every distance to examine the system response. Every test was made with the PID-parameters which provided the step response in Chapter 4.2.

4.4 Results

4.4.1 Noise with Kalman filter

While the sensor was kept still, the noise from the sensor after filtering could be examined. The sample time was 10ms.

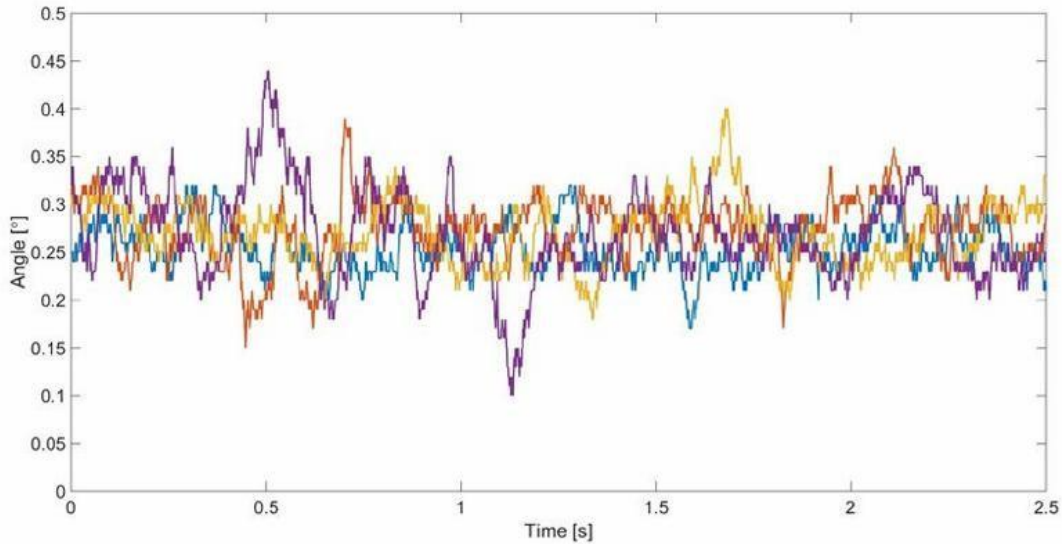


Figure 12. Plot showing the angles values for the sensor using the Kalman filter. The result is shown in Figure 12. The four graphs represent one test each. A stable output equals a low amount of noise.

The mean value for the four tests is 0.27° with a maximum value of 0.44° and a minimum value of 0.10° . The biggest difference from the mean is 0.17° , which is within the requirements.

4.4.2 Step info

More information about the step responses for the two subsystems in Figure 10 was provided from MATLAB. The values interesting for the result was the rise time, the overshoot, the settling time and the steady state error.

	Motor A	Motor B	Requirements
Rise time	0.75	0.70	< 1 s
Overshoot	0.8 %	0.9 %	< 2 %
Settling time	1.35	1.30	< 2 s
Steady state error	0.57°	0.57°	< 1°

Table 3. Step information for the two sub systems.

As seen in Table 3 the requirements for the systems, which were set in Chapter 4.2, were fulfilled.

	K_P	K_I	K_D
Controller A	12.14	0.56	23.46
Controller B	12.64	0.62	23.48

Table 4. Table with the PID-parameters for controller A and controller B.

The PID-parameters for both systems which fulfilled the requirements are shown in Table 4.

4.4.3 Asymmetrically placed load

The results from the test with the asymmetrically placed load can be seen below.

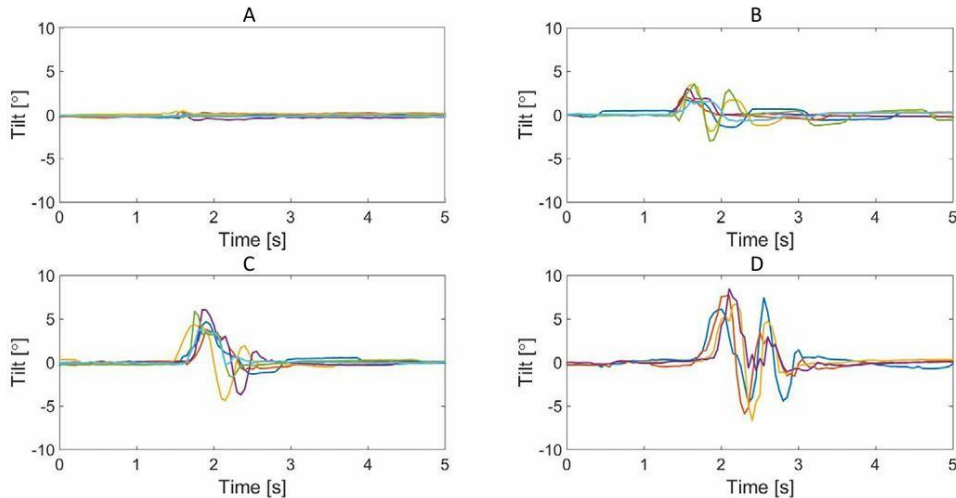


Figure 13. Plots showing the angular fluctuation over time when the load is put on the platform in four different positions, A, B, C and D. In Figure 13 the tilt in degrees ($^{\circ}$) in both planes, over time (s), is shown. In plot A the load is put at the center of the platform. In plot B the load is moved a bit towards the corner at the platform, plot C even closer, and in plot D it is placed in the corner of the platform, at the same distance from the IMU in x- and y-direction.

The load is put at the platform at $t = 1.5s$, and this is when the disturbance first occurs in the plots. The disturbance in plot A is close to zero, and then increased when moving the load closer to the corner. The largest disturbance can be seen in plot D where the load is in the corner of the platform.

In all four tests the steady state error is within the required limits.

5. DISCUSSION AND CONCLUSIONS

In this chapter the previous yielded results are analyzed and summarized. Possible error sources are discussed, as well as the conclusions.

5.1 Discussion

5.1.1 Kalman filter

The result in Figure 12 shows that the filter provides a signal which contains some noise.

However, with an arm as short as the one used in the demonstrator, minor disturbances may not be of a problem for the model since it would generate such small movements at the top. The result was considered satisfying and no other filters were tested.

5.1.2 PID and step response

Since the overshoot is much smaller than the allowed value there is a chance that the speed of the system could be improved and still have a step response within the requirements.

If the sample time in the discrete time domain is reduced, the system would most likely be easier to control. More tests have to be done to determine if the chosen sample time gives the most efficient control.

5.1.3 Asymmetrically placed load

When placing a load in the center of the platform, both the angular deviation and the static error are small. The further the load is moved from its theoretical placement the more the system starts to overshoot. This is because the model does not expect the torque or the increased moment of inertia that an asymmetrical placed load generates.

However, the accuracy of the model cannot be evaluated by this test since the step made in Figure 10 is made for a step of 11.4 °, and no corresponding test has been done for the demonstrator. The test can only answer how the system reacts when an asymmetrical load is used. For evaluations of how well the theoretical model corresponds to the demonstrator, other tests are required.

A different placement from the theoretical model is likely not the only reason to the bad output in test B, C and D. The DC-motor has no natural hold-torque ability like a stepper motor has (Wevers et al, US 4679102 A) and is best suited for continuous rotation.

Multiple tests were made at every distance and in Figure 13 some divergence between these tests can be seen. This may depend on a slightly different placement for the load in the tests.

5.1.4 Possible error sources

Simplifications have been made regarding the movement of the platform. The demonstrator moves in space, but the movement from each motor is seen as movement in one plane. Therefore the model does not consider motion of the center of mass, other than in its own plane.

The theoretical model does not consider static friction. This is perceived as one of the main error sources. Since the motors often compensate for small angular fluctuation, the friction in the motor will most likely affect the required torque considerably. The static friction is not linear, which is why it cannot be considered in the transfer function.

Other error sources include:

- The resistance may differ $\pm 12\%$ according to the data sheet
- The grip of the naves may not be perfect
- The platform might sag slightly from a load
- Noise from the sensor

5.2 Conclusions

By performing tests on the demonstrator the research questions could be answered.

How will the system reply to a load put on the platform asymmetrically?

The result from Chapter 4.4 shows that the system stays stable when the load is put in the center, and that the static error is small. Other placements will make the system behave in a way which cannot be predicted from the model. When the load is moved from the center, the fluctuation increases and it takes longer time for the system to recover from the disturbance and return to steady state.

Can the imbalance be compensated for?

The demonstrator compensates for the caused imbalance but slower than when the load is put in the center. Longer distance between the load and the center, results in bigger fluctuation and longer time to return to steady state. The steady state error however is within the requirements for all four distances.

6. RECOMMENDATIONS AND FUTURE WORK

In this chapter recommendations for the project are submitted. It also contains ideas about what would be done in this project if future work would be done.

6.1 Recommendations

For anyone interested in the subject of stabilizing platforms it is recommended to take benefit from the huge Arduino Open-Source community. It has contributed with lots of pre made software to make the usage of an IMU easier. By doing so, focus can be put on making an accurate model with a fast and robust controller.

It is also highly recommended to consider the choice of motor type carefully depending on the range of use for the platform. If the usage involves a load which requires a hold torque to keep it horizontal, a DC-motor may not be a good choice even with an accurate controller.

6.2 Future work

For future work, the system, as well as the demonstrator itself, could be improved in many aspects.

To improve both the speed and robustness of the system another controller than PID could be implemented. A state-space controller could possibly give better results since it is controlling the system dynamically. However, this requires a more accurate model of the system which was hard to achieve without using the MATLAB application Simulink, since the static friction otherwise has to be neglected.

A Simulink-model would have contributed with the possibility to add the static friction from the motor which is listed as one of the main error sources. It would also give the opportunity to add simulations of noise to verify the models probability.

Some changes regarding the demonstrator can be done. By reconsidering the choice of motor the system might be improved. For example, stepper motors are more capable of handling static torque which can increase how much load the system can handle.

Further on, the speed of the system could be improved. As seen, the step response fulfill the requirements; yet, the system could be made even faster by optimizing the software. For example, the Kalman filter is an algorithm which is very complex. If using a simpler filter the runtime of the system could be reduced. For example, a complimentary filter might fulfill the requirements with less calculation (Higgins, 1975, 325) which will make it possible to lower the sample time of the system.

REFERENCES

- Arduino, 2015. Arduino – Rotary Encoders. Available at:
<http://playground.arduino.cc/Main/RotaryEncoders>, [Accessed: 2015-05-03] Arduino,
2015. Datasheet – Keyes L298 Motor driver. Available at:
<https://arduinoinfo.wikispaces.com/file/view/L298-2.pdf/281104616/L298-2.pdf>.
[Accessed: 2015-0412]
- Arduino Uno, 2015. Arduino – ArduinoBoardUno. Available at:
<http://arduino.cc/en/main/arduinoBoardUno>, [Accessed: 2015-02-19] Atmel,
2015. Data sheet – Atmega32. Available at:
<http://www.atmel.com/devices/atmega32.aspx>. [Accessed: 2015-03-03]
- Because We Can! labs, 2014. CoffeeMate - Arduino controlled self-stabilizing platform,
gyro / accelerometer as sensors. Available at:
<https://www.youtube.com/watch?v=EbMFuhaoxpo>. [Accessed: 2015-02-17]
- Danapalasingam K. A., Leth J., la Cour-Harbo A., and Bisgaard M., 2010. Robust
Helicopter Stabilization in the Face of Wind Disturbance. Available at:
http://ieeexplore.ieee.org/xpls/abs_all.jsp?arnumber=5717418. [Accessed: 2015-05 05]
- Dimension Engineering, 2015. A beginner's guide to accelerometers. Available at:
<http://www.dimensionengineering.com/info/accelerometers>. [Accessed: 2015-03-20]

Electrokit, 2015. Nave datasheet. Available at:

<http://www.electrokit.com/hub02universellt-nav-6mm-par.44888> [Accessed:2015-02-21]

Escorts Heart Institute and Research Centre, New Delhi, India, Journal of Cardiothoracic and Vascular Anesthesia, Volume 16, Issue 6, December 2002, Pages 685–690. Available at: <http://www.sciencedirect.com/science/article/pii/S1053077002001234> [Accessed: 2015-04-27]

Faragher, Ramsey, 2012. Understanding the Basis of the Kalman Filter Via a Simple and Intuitive Derivation. IEEE Signal Processing Magazine. Available at:

<http://www.cl.cam.ac.uk/~rmf25/papers/Understanding%20the%20Basis%20of%20the%20Kalman%20Filter.pdf>. [Accessed 2015-03-05]

Faulhaber, 2015. Data sheet - Planetary Gearhead Series 23/1. Available at:

https://fmcc.faulhaber.com/resources/img/EN_23-1_FMM.PDF. [Accessed: 2015-03-04]

Glad, T. and Ljung, L., 2014. Reglerteknik – grundläggande teori. Studentlitteratur AB.

Gosselin, St-Pierre, 2003. Development and Experimentation of a Fast 3-DOF Camera Orienting Device. Available at: <http://ijr.sagepub.com/content/16/5/619.short>, [Accessed: 2015-04-03]

Higgins, W. T. Jr., 1975. A Comparison of Complementary and Kalman Filtering. Member, IEEE, Arizona State University, Tempe, Ariz. 85281. Available at:

https://proyectos.ciii.frc.utn.edu.ar/cuadricoptero/export/9ed95816c90cc7d83e32fd2e13b032dc515c0d7a/documentacion/articulo_case_filtro_comp/referencias/A%20comparison%20of%20complementary%20and%20kalman%20filtering.pdf. [Accessed: 2015-05-12]

Institut für Theoretische Elektrotechnik und Systemoptimierung, Universität Karlsruhe, Kaiserstr. 12, D-76128 Karlsruhe, Germany, 2006. An integrated GPS/MEMS-IMU navigation system for an autonomous helicopter. Available at:

http://ac.elscdn.com/S1270963806000484/1-s2.0-S1270963806000484main.pdf?_tid=426eb69af7d9-11e4-9735

00000aab0f26&acdnat=1431347502_d826dff7933c69c0b57e566441853bf9 [Accessed:

2015-04-13]

InvenSense, 2012. Datasheet – MPU 9150. Available at:

<http://dlnmh9ip6v2uc.cloudfront.net/datasheets/Sensors/IMU/PS-MPU-9150A.pdf>.

[Accessed: 2015-02-19]

Johansson H. et al, 2010. Elektroteknik. KTH

Kleeman, L. 1996. Understanding and Applying Kalman Filtering. Department of Electrical and Computer Systems Engineering Monash University. Available at:

Clayton <http://www.ecse.monash.edu.au/centres/irrc/LKPubs/Kalman.PDF> [Accessed: 2015-04-02]

Kleeman, L. 1996. Understanding and Applying Kalman Filtering. Department of Electrical and Computer Systems Engineering Monash University. Available at:

Clayton <http://www.ecse.monash.edu.au/centres/irrc/LKPubs/Kalman.PDF> [Accessed: 2015-04-02]

Liu, Qiang Zhu, Howe, 2006. Instantaneous Torque Estimation in Sensorless Direct Torque-Controlled Brushless DC Motors. Available at:

<http://ieeexplore.ieee.org/stamp/stamp.jsp?tp=&arnumber=1703721>, [Accessed: 2015-05-07]

MathWorks, 2012. DC Motor Position: System Modeling. Available at:

<http://ctms.engin.umich.edu/CTMS/index.php?example=MotorPosition§ion=SystemModeling>. [Accessed: 2015-02-01]

Michigan Tech, 2015. Faulhaber datasheet, DC-micromotors. Available at:

http://www.me.mtu.edu/~wjendres/ProductRealization1Course/Motor_Specs.pdf. [Accessed: 2015-03-03]

Paller, 2012. Better motion control using accelerometer/gyroscope sensor fusion.

Available at: <http://www.slideshare.net/paller/better-motion-control-using-accelerometergyroscope-sensor-fusion>. [Accessed 2015-03-25]

Pan, S. and Pal, J., 1995. Reduced order modelling of discrete-time systems. Department of Electrical Engineering, Indian Institute of Technology, Kharagpur, India. Available at:

http://ac.els-cdn.com/0307904X94000104/1-s2.0-0307904X94000104main.pdf?_tid=d56ec19e-f7dc-11e4-a55c00000aab0f26&acdnat=1431349037_4750f38c80e262a0693be2fb9635a292 [Accessed: 2015-05-02]

Rivello, 2011. Self-Stabilizing Platform using Arduino, Accelerometer and Gyroscope. Available at: <https://www.youtube.com/watch?v=TOSFAdPUUYs> [Accessed: 2015-02-15]

Ruderman, M., Krettek, J., Hoffmann, F. and Bertram, T., 2008. Optimal State Space Control of DC Motor. The International Federation of Automatic Control. Available at: <http://scl.hanyang.ac.kr/scl/database/papers/IFAC/2008/data/papers/3625.pdf> [Accessed: 2015-03-20]

Ruderman, M., Krettek, J., Hoffmann, F. and Bertram, T., 2008. Optimal State Space Control of DC Motor. The International Federation of Automatic Control. Available at: <http://scl.hanyang.ac.kr/scl/database/papers/IFAC/2008/data/papers/3625.pdf> [Accessed: 2015-03-20]

Virgala, I. and Kelemen, M., 2012. Experimental Friction Identification of a DC Motor. Available at: <http://article.sapub.org/pdf/10.5923.j.mechanics.20130301.04.pdf> [Accessed: 2015 05-02]

Weisstein, Eric W. Covariance. From MathWorld--A Wolfram Web Resource. Available at: <http://mathworld.wolfram.com/Covariance.html>. [Accessed: 2015-04-01] Åström, K. J. and Murray, R. M., 2004. Analysis and Design of Feedback Systems, Preprint. Available at: <http://www.cds.caltech.edu/~murray/courses/cds101/fa04/reading.html> [Accessed: 2015-04-16]